Scientific Research Publishing

Open Journal of Applied Sciences, 2026, 16(2), 593-607
https://www.scirp.org/journal/ojapps
ISSN Online: 2165-3925
ISSN Print: 2165-3917

Comparative Study between Functionalized and Nanoparticle Decorated Carbon Nanotube as Reinforcing Filler in Epoxy Matrix

Akhilesh Singh[1], Anurag Mishra[1], Deep Narayana Maurya[2], Ashutosh Singh[1], Abhishek Singh[3], Anil Kumar Soni[4*]

[1]Department of Chemistry, K. S. Saket P.G. College Ayodhya, Faizabad, India
[2]Department of Chemistry, D.N College Meerut, Meerut, India
[3]Department of Chemistry, U.P. Autonomous College, Varanasi, India
[4]Department of Chemistry, Shia Post Graduate College, Lucknow, India
Email: akhileshchem@gmail.com, anuragm878@gmail.com, mauryadeep343@gmail.com, asinghkssaket@gmail.co, abhupc@gmail.com, *anilsony82@gmail.com

How to cite this paper: Singh, A., Mishra, A., Maurya, D.N., Singh, A., Singh, A. and Soni, A.K. (2026) Comparative Study between Functionalized and Nanoparticle Decorated Carbon Nanotube as Reinforcing Filler in Epoxy Matrix. *Open Journal of Applied Sciences*, **16**, 593-607.
https://doi.org/10.4236/ojapps.2026.162037

Received: January 9, 2026
Accepted: February 11, 2026
Published: February 14, 2026

Abstract

In this investigation, two distinct varieties of multi-walled carbon nanotubes (MWCNTs) were employed: specifically, functionalized carbon nanotubes modified with 3-Aminopropyltriethoxysilane (MWCNT/APTES) and carbon nanotubes adorned with titanium dioxide nanoparticles (MWCNT/TiO_2). These nanomaterials were meticulously integrated into an epoxy matrix using ultrasonication. The central objective was to evaluate the capability and role of these reinforced carbon nanotubes in epoxy matric to withstand under various applied stresses. This study presents findings on the influence of MWCNT/APTES and MWCNT/TiO_2 to enhance the tensile and dynamic mechanical performance of epoxy nanocomposites. The morphology of the newly formed MWCNT/APTES and MWCNT/TiO_2 was scrutinized through TEM. FESEM analysis of the tensile fracture surface validates the efficient dispersion of TiO_2 assisted MWCNTs within the epoxy. The outcomes suggest that when employing nanoparticle-decorated carbon nanotubes to reinforce the epoxy matrix, stress transfer transpires more effectively from the matrix to the reinforcement in comparison to the use of functionalized carbon nanotubes. For instance, with the addition of 1.5 wt.% MWCNT/TiO_2 nanofillers, the storage modulus of the epoxy increased to 1380 MPa, compared to 1156 MPa for neat epoxy.

Keywords

Carbon Nanotubes, Epoxy Nanocomposites,
Titanium Dioxide Nanoparticles, Surface Functionalization,
Dynamic Mechanical Analysis

1. Introduction

Epoxy is a two-component system that forms through a cross-linking process, However, it's worth noting that this cross-linking process introduces some brittleness to epoxy, which can limit its applicability. To address the brittleness issue associated with epoxy, various nanofillers are incorporated into the epoxy matrix [1]-[4]. Among these, carbon nanotube (CNT)stands out as a particularly promising candidate due to its combination of exceptional superior mechanical, electrical and thermal performance and garnering significant attention across various research domains [4]-[6]. These properties make carbon nanotubes (CNTs) suitable for a wide range of applications, including the creation of nanocomposites for enhanced conductivity and strength [7] [8], electromagnetic interference shielding, energy conversion devices sensors, hydrogen storage, and nanoscale semiconductor devices [9]-[11]. Moreover, there is a growing interest among researchers in utilizing carbon-based nanocomposites for biomedical applications [12]-[16].

A significant challenge associated with carbon nanotubes is their tendency to aggregate within a polymer matrix, driven by factors such as their inter-tubular van der Waals and pi-pi forces interaction forces with high specific surface area [17]-[21]. These clusters hinder their effectiveness as a perfect filler for polymer matrix. Furthermore, the interaction between CNTs and polymers can impact dispersion, which is crucial for efficiently transferring of applied stress from polymer long chain molecule to CNTs. Various strategies have been employed to address these issues, including functionalization of CNTs and casting through high-energy ball milling, Twin Screw Extrusion,3-roll milling, and ultrasonication [22]-[24].

It's essential to note that while functionalizing carbon nanotubes can improve dispersion [25]-[28], it may also compromise their atomic structural perfection, potentially affecting their performance [29] [30]. The use of dispersing aid solvents can enhance dispersion but often involves the time-consuming removal of solvents, which may introduce voids in the composite, adversely affecting mechanical properties [31].

The presence of nanoparticles during the dispersion of CNTs in polymer matrix also assists the dispersion of CNTs. These composite materials retain their inherent properties and exhibit synergistic effects. Various methods have been reported to decorate the surface of CNT with inorganic nanoparticles, and consider the sol-gel process as a potential method [32], these obtained hybrid nanomaterials have

been applied to applications related to photocatalysis and optoelectronics [33]-[35]. In such applications, establishing good electronic contact between CNTs and nanoparticle is essential, often involving chemical modifications to the CNT surface. In the present study, functionalized MWCNTs (MWCNT/APTES) and MWCNTs decorated with TiO_2 nanoparticles were utilized to achieve superior performance at higher weight percentages (1.5 wt.%) in an epoxy matrix.

2. Experimental

2.1. Materials

Resin and an amine-based hardener were sourced from Huntsman. The TiO_2 nanoparticles, with a diameter of approximately 40 nm, and multi-walled carbon nanotubes, with a diameter of around 38 nm, were synthesized using the sol-gel and chemical vapor deposition (CVD) methods, respectively.

2.2. Functionalization of MWCNTs with 3-Aminopropyltriethoxysilane (APTES)

To enhance the surface compatibility of MWCNTs with epoxy matrix, functionalization with 3-Aminopropyltriethoxysilane (APTES) was performed. The procedure consisted of several steps as outlined below:

2.3. Chemical Oxidation of MWCNTs

The functionalization process began with 0.5 grams of CVD-synthesized MWCNTs. The MWCNTs were refluxed in an 80 ml mixture of H_2SO_4 and HNO_3 in a 3:1 ratio for 4 hours at 70˚C. After refluxing, the MWCNTs modified with -COOH groups were collected by filtration and washed repeatedly with distilled water until the pH reached 7. The modified MWCNTs underwent two washes with acetone to eliminate any trapped water inside the bundles of MWCNTs. Finally, the functionalized MWCNTs were placed in a vacuum oven at 110˚C overnight to ensure complete drying (**Figure 1**).

2.4. Chlorination of MWCNTs

The MWCNTs with -COOH groups were placed in a 100 ml round bottom flask along with 40 ml of thionyl chloride ($SOCl_2$). The mixture was refluxed for 30 hours under an inert atmosphere of nitrogen gas and filtered. The solid residue, which consisted of chlorinated MWCNTs, was washed several times with anhydrous tetrahydrofuran (THF) to remove any residual reactants and dried at 50˚C overnight, resulting in the modified MWCNTs, which were designated as MWCNT/COCl (**Figure 1**).

2.5. APTES Functionalization

In the final step of the functionalization process, approximately 0.5 grams of MWCNT/COCl was suspended in dry tetrahydrofuran (THF) along with an excess of 3-Aminopropyltriethoxysilane (APTES). The mixture was refluxed for ap-

proximately 90 hours, allowing APTES groups to be introduced onto the surface of MWCNTs. After silylation, the functionalized MWCNTs (designated as MWCNT/APTES) were washed with ethanol to remove excess amine and then with deionized water to ensure thorough cleaning. The MWCNT/APTES were dried under vacuum before use. The all steps of this procedure are visually illustrated in Figure 1.

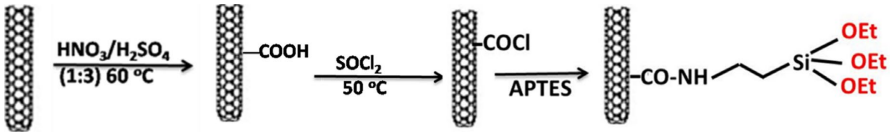

Figure 1. Pictorial view of chemical reaction during functionalization of MWCNTS with APTES.

2.6. Attachment of TiO_2 Nanoparticles on the Surface of MWCNTs

A blend of Multi-Walled Carbon Nanotubes (MWCNT/TiO_2) weighing 0.20 grams and Titanium Dioxide (TiO_2) nanoparticles weighing 0.10 grams was subjected to sonication at 50% amplitude with a 5-second on and 5-second off pulse in 100 ml of acetone. This sonication process was carried out for 4 hours at room temperature. The resulting MWCNT/TiO_2 blend was dried for a period of 10 hour sat 100˚C in a vacuum oven (Figure 2).

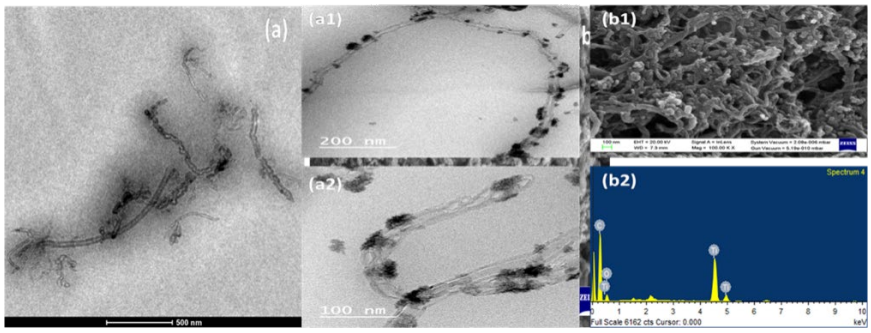

Figure 2. TEM images of functionalize MWCNTs (a) and nano particles decorated MWCNTs (a1) and (a2), and fesem image nano particles decorated MWCNTs (b1) and (b2).

2.7. Casting of Nanocomposites

The MWCNTs (1.5 wt.%) was thoroughly mixed with epoxy resin and 15% acetone using a glass rod. Ultrasonic waves at 50% amplitude were applied to this mixture, which had a volume of 50 ml, for a duration of 45 minutes. External cooling was employed during this process to prevent an increase in temperature and then vaporized the acetone solvent at 60˚C for a duration of 12 hours.

Subsequently, 10 wt.% of amine-basedhardener was uniformly mixed into the mixture of epoxy resin and MWCNTs, and finally cast into a silicone rubber mold to prepare sample testing specimens. The mold with the epoxy resin mixture was placed in a hot air oven at 70˚C for 10 hours to allow the epoxy resin to cure. The

same process was followed for the reinforcement of MWCNT/APTES in epoxy matrix (Figure 3).

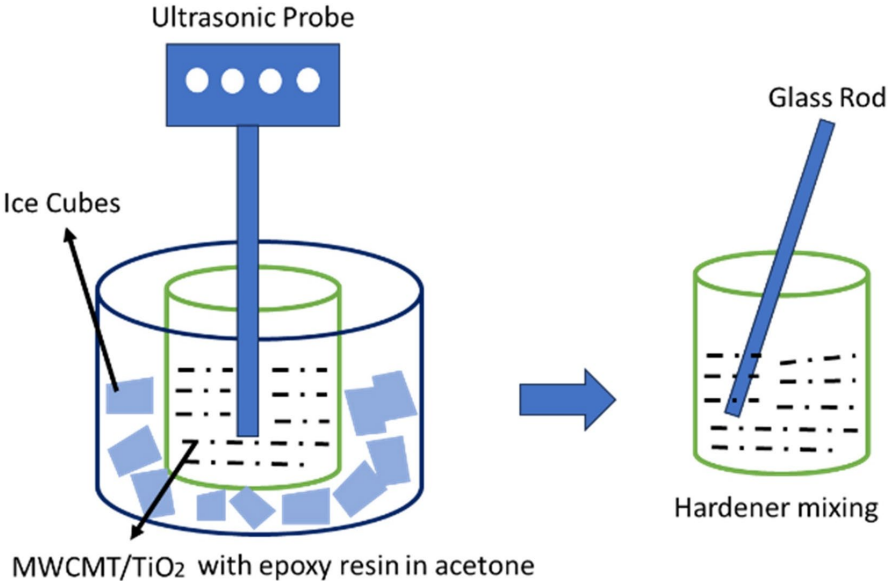

Figure 3. A schematic illustration of the preparation of nanocomposite.

2.8. Characterization

The dispersion of nano reinforcements in the matrix and the identification of toughening mechanisms on the tensile fracture surface were investigated using a Field Emission Scanning Electron Microscope (FESEM, Zeiss) (acceleration voltage -15 kV). The surfaces of the samples were coated with gold to enhance imaging quality.

Transmission Electron Microscopy (TEM) was utilized to study the morphology of MWCNT/APTES and MWCNT/TiO_2. A small drop of the epoxy resin containing the fillers (MWCNT/APTES or MWCNT/TiO_2), after the sonication process, was used for the analysis. A copper grid coated with carbon, typically with a mesh size of 200, was chosen as the substrate for mounting the sample. The TEM analysis was conducted using the FEI Technai G2-20-S-Twin microscope.

The tensile testing of nanocomposite samples adhered to the ASTM D-638(V) standard. We used dumbbell-shaped tensile specimens and examined them with a Hounsfield Universal Testing Machine (model H25KS). The testing was carried out at a crosshead speed of 1 mm per minute, conducted under normal ambient conditions. To ascertain the tensile strength and elastic modulus, we analyzed stress-strain curves. Each composition underwent testing with a minimum of five replicate specimens, and we reported the average values along with their respective standard deviations.

Cast specimens of neat epoxy and its nanocomposite were prepared to precise dimensions of 9.2 × 7.5 × 2.5 mm^3 through fine emery paper polishing. This was done in accordance with the requirements of single cantilever bending mode dynamic testing. Perkin-Elmer DMA 8000 was used for dynamic mechanical analysis from 35 to 180˚C at 1 Hz as per ASTM D4065.

3. Results and Discussions

3.1. FTIR Spectra Analysis

The molecular structural characteristics of the MWCNT/APTES and MWCNT/TiO_2 were assessed using Fourier transform infrared (FTIR) spectroscopy. To begin, MWCNT/APTES as well as MWCNT/TiO_2 were blended with high-purity potassium bromide (KBr, Aldrich, 99.9%) and compacted using a 10-ton load in a die to create a film suitable for infrared analysis. The infrared spectra were then recorded under normal ambient conditions using an FTIR spectrometer, specifically the Thermo Nicolet Nexus 1600. Figure 4 displays the FTIR spectra of APTESfunctionalized MWCNTs and TiO_2 nanoparticles decorated MWCNTs.

In FTIR spectra of MWCNT/APTES (Figure 4(a)), the broad band at 3411 cm^{-1} corresponds to the stretching vibration of –OH groups. The peak at 1640 cm^{-1} is associated with the presence of carbon-carbon double bond (C=C) network in MWCNTs and also with C=O of amide (broad peak) groups attached to MWCNTs. The absorption at wavenumber 1330 cm^{-1} and 1073 cm^{-1} are attributed to the -Si-O- and -N-C- amide groups, respectively. The peaks at 2922 cm^{-1} and 2855 cm^{-1} are assigned to the –C-H stretching vibration of ethylene, which is produced at the defect sites of MWCNTs after acid treatment. These peaks indicate acid functionalization and confirm the presence of APTES on the surface of MWCNTs. This FTIR analysis provides valuable information about the functionalization of MWCNTs with APTES and the resulting chemical changes in the material, which is important for understanding their properties and compatibility in the epoxy nanocomposites.

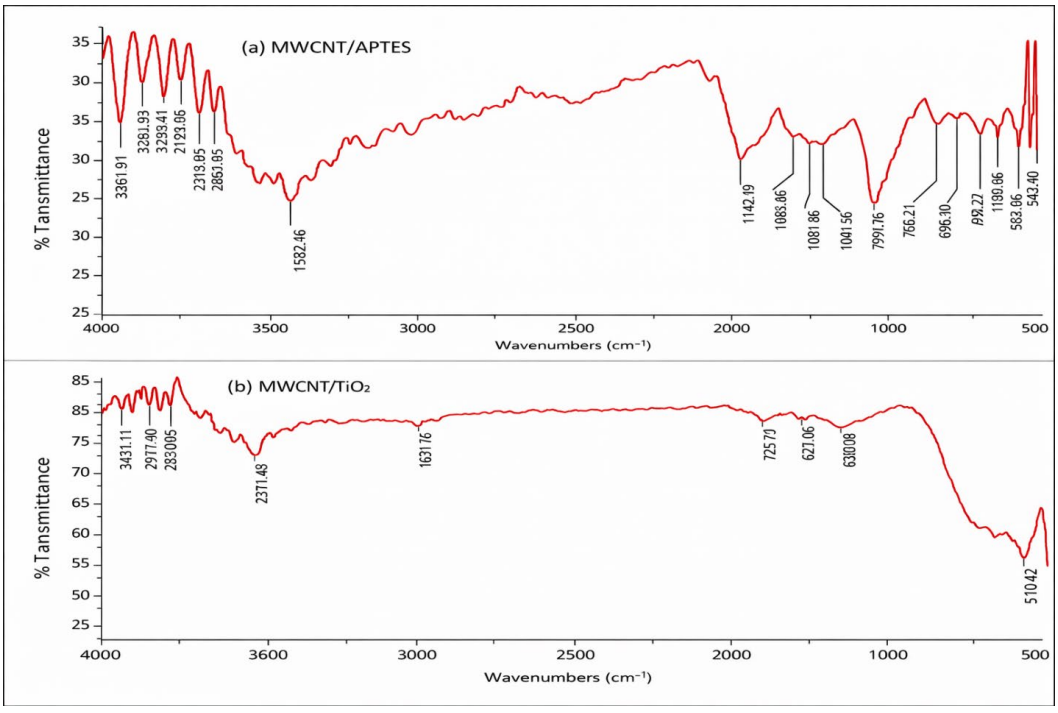

Figure 4. (a) FTIR spectra MWCNT/APTES; (b) FTIR spectra of MWCNT/TiO_2.

In the FTIR spectra of TiO_2 nano particles decorated MWCNTs, the broad peak observed at 3425 cm^{-1} can be ascribed to the presence of -OH groups in both MWCNTs and TiO_2. The peaks corresponding to the -Ti-O- network in the Rutile phase of TiO2 were observed at 1113 cm^{-1} and 515 cm^{-1}. here it is noted that, this FTIR spectra reveals the presence of all the characteristic peaks associated with MWCNTs. However, a significant shift in the stretching frequency of the -C=C- framework of MWCNTs is evident, moving from 1630 cm^{-1} to 1571 cm^{-1} (as depicted in **Figure 4**). This shift in frequency is attributed to the bonding of TiO_2 nanoparticles onto the surface of MWCNTs [36]. This bonding results in a form of back bonding, where Ti metal interacts with the anti-bonding molecular orbital of the -C=C- groups in CNTs. This shift in the FTIR spectrum signifies the interaction between CNTs and TiO2, shedding light on the chemical alterations and bonding that occur within the MWCNT/TiO_2 nanocomposite.

3.2. Tensile Strength and Elastic Modulus

Tensile testing was conducted to generate stress-strain curves for both the epoxy and its nanocomposites. These nanocomposites included 1.5 wt.% loading of various MWCNT types (MWCNT/APTES and MWCNT/TiO_2). The outcomes of this testing are depicted in **Figure 5**. Analysis of these curves allowed for the calculation of the materials' tensile strength and elastic modulus. The tensile characteristics of the epoxy as well as nanocomposites, such as tensile strength and elastic modulus, are provided in **Table 1**. This data provides valuable insights into the mechanical behavior and performance of the epoxy nanocomposites, especially in comparison to the pure epoxy. The introduction of 1.5 wt.% of MWCNT/TiO_2 into the epoxy matrix results in a significant enhancement of both tensile strength and elastic modulus. Specifically, these properties increase by approximately 20% and 18%, respectively, in comparison to the pure epoxy.

The enhancement in mechanical properties of any nanocomposite can be attributed to the uniform distribution of nanofiller within the polymer matrix. This even dispersion, coupled with effective interfacial interactions, plays a pivotal role in elevating the material's performance. The substantial improvement observed in tensile strength and elastic modulus of MWCNT/TiO_2 epoxy nanocomposite is primarily a result of the nearly individual dispersion of MWCNT/TiO_2 throughout the epoxy matrix (**Figure 6**). This dispersion leads to an increased surface area available for interaction with the epoxy, consequently restraining the mobility of epoxy chains and facilitating the transmission of stress from the epoxy matrix to MWCNT/TiO_2.

The inclusion of 1.5 wt.% of MWCNT/APTES in the epoxy likewise leads to enhancements in both tensile strength and elastic modulus, although the increases are relatively lower, approximately around 11% and 8%, respectively, in comparison to the pure epoxy. It's worth noting that there is a lack of uniformity in the improvement, as evident from the relatively significant data deviations.

The variation in performance may be due to the presence of clusters of MWCNT/APTES in the epoxy matrix, caused by MWCNT-MWCNT interactions. These clusters act as defects in the MWCNT-epoxy nanocomposite and result in poor interaction between the MWCNTs and the epoxy matrix, leading to a degradation of mechanical performance and increased deviation. These observations highlight the importance of achieving a homogeneous dispersion of MWCNTs in the epoxy matrix for optimal mechanical performance. The presence of clusters or agglomerates of MWCNTs can negatively impact the properties of the nanocomposite, underscoring the need for effective dispersion strategies to harness the full potential of MWCNTs in enhancing material performance.

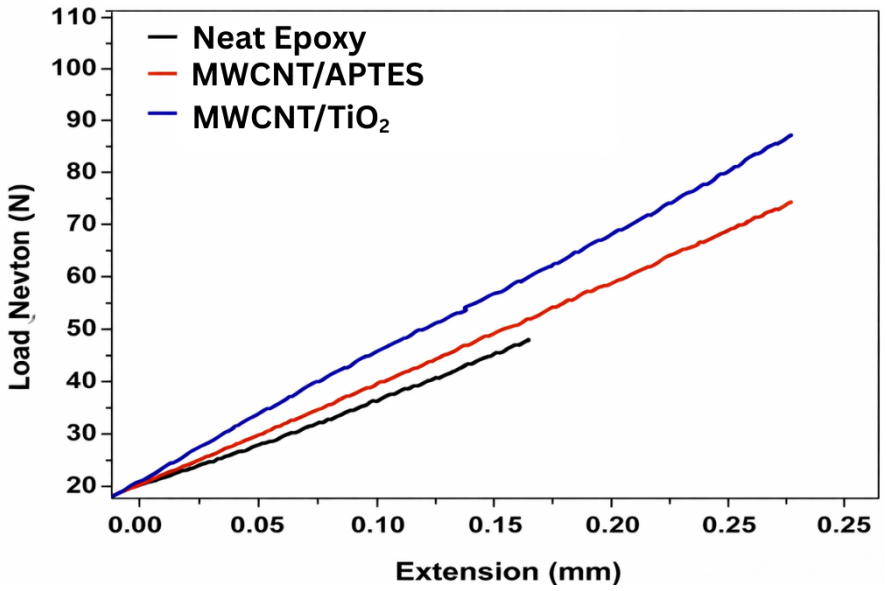

Figure 5. Stress-strain curves of epoxy, MWCNT/APTES epoxy nanocomposite and MWCNT/TiO_2 epoxy nanocomposites.

Table 1. Tensile strength, elastic modulus, storage and glass transition temperature (Tg) of epoxy, MWCNT/APTES epoxynanocomposite and MWCNT/TiO_2 epoxynanocomposite (1.5 wt.%).

Nanocomposites	Tensile Strength (MPa)	Elastic Modulus (GPa)	Storage modulus at 35˚C (MPa)	Tg (˚C)
Epoxy	54 ± 1.4	6.1 ± 0.04	1156	75
MWCNT/APTES	60 ± 1.3	6.6 ± 0.01	1230	80
MWCNT/TiO_2	65 ± 0.7	7.2 ± 0.03	1380	84

3.3. Tensile Fracture Surface Analysis

Figure 6 presents FESEM images of tensile fracture samples for both the pure epoxy and its nanocomposites. In Figure 6, the direction of crack propagation is indicated by single-headed red arrows. In both the pure epoxy and its nanocom-

posites, we observed three distinct fracture zones on the tensile fracture surface throughout the entire process of fracture, from the initial stage to the completion of fracture. These zones are referred to as the mirror zone, the mist zone, and the hackle zone on the tensile fracture surfaces. Within the mirror zone, cracks initiate and progress at a relatively slow pace before rapidly accelerating, leading to exceptionally smooth fracture surfaces. The immediate vicinity of the mirror zone, characterized by slight roughness and a thin region, is termed the mist zone. Surrounding the mist zone is the hackle zone, which exhibits a rough and thicker region (**Figure 6**).

In **Figure 6(a2)**, we observe the mirror zone of the tensile fracture surface at a higher level of magnification. The fracture surface of the pure epoxy is distinctly visible, featuring exceptionally smooth and river-like patterns. In this region, cracks appear to propagate freely and randomly, indicating the inherent vulnerability of the pure epoxy to crack initiation and propagation. This behavior is characteristic of a typical brittle fracture.

Nevertheless, when 0.1 wt.% of MWCNT/TiO_2 is introduced, the fracture surface undergoes a transformation, becoming rough with the presence of numerous winding and deep cracks within the mirror zone (as depicted in **Figure 6(b1)** and **Figure 6(b2)**). Typically, increased roughness signifies the dissipation of more fracture energy. These observations suggest the creation of a new fracture surface due to the deflection of crack fronts.

The FESEM image (**Figure 6(c3)**) of fracture surface of MWCNT/TiO_2 epoxy nanocomposite at higher magnification in mirror zone shows uniformly dispersion of MWCNTs in epoxy without formation of clusters of MWCNTs. The well dispersion of MWCNTs in the epoxy matrix offers large number of obstacles to the crack propagation and generates more number of crack deflection paths in epoxy matrix and leads to enhancement in the performance of MWCNT/TiO_2 epoxy nanocomposite. The FESEM images of tensile fracture surface of MWCNT/APTES epoxy nanocomposite in mirror zone at higher magnification also confirmed that the dispersion of MWCNTs become worsen and some clusters of MWCNTs are formed in epoxy (**Figure 6(c2)**) at loading of MWCNTs (0.1 wt.%). The presence of cluster of MWCNTs in epoxy matrix generally acts as defect and diminishes the mechanical and physical properties of polymer nanocomposite. So, it is clearly observed that crack deflection is mainly occurred in case of MWCNT/TiO_2 epoxy nanocomposite compared to MWCNT/APTES epoxy nanocomposite, due to better MWCNTs dispersion in earlier one. The FESEM image of MWCNT/TiO_2 epoxy nanocomposite at high magnification in mirror zone (**Figure 6(b2)**) shows a range of toughening mechanisms, like crack may propagate through the polymer matrix above or below the poles of the MWCNTs resulting in the more energy consumption due to crack deflection [37]. Crack bridging mechanism, which occurs when a crack propagates and found a MWCNTs right in front of its path resulting the bridging of the crack [38].

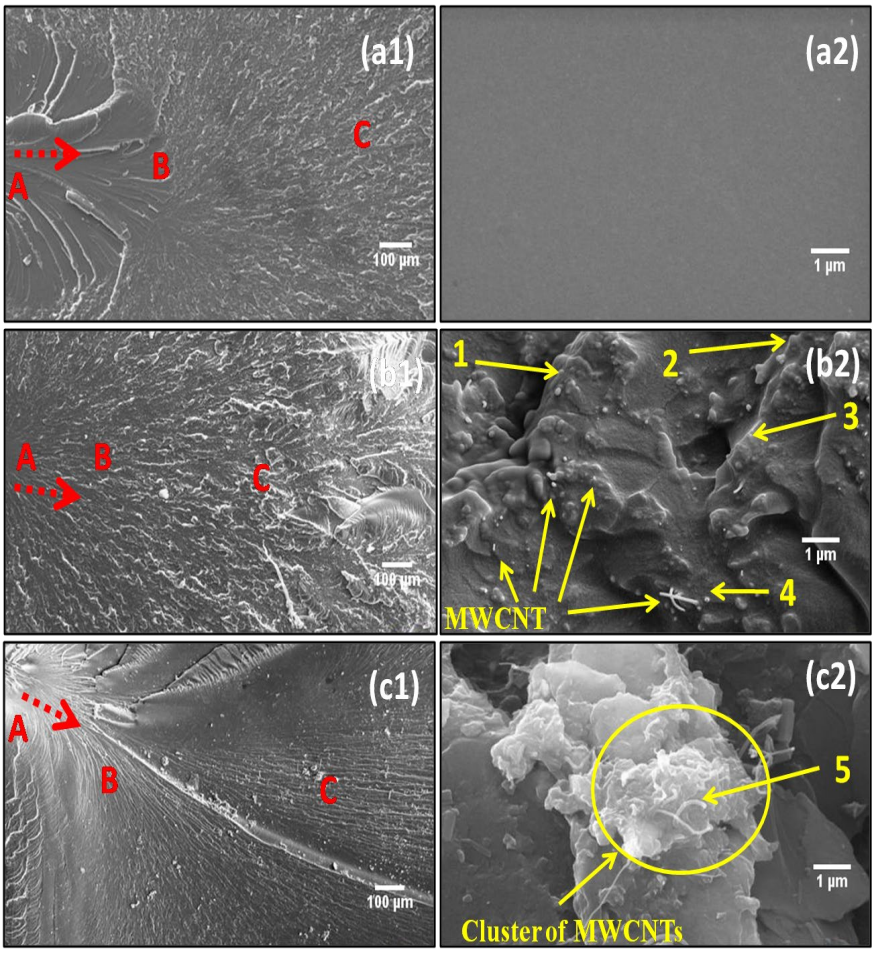

Figure 6. FESEM images of (a1) neat epoxy, (a2) neat epoxy (High magnification of mirror zone), (b1) MWCNT/TiO_2 epoxy, (b2) MWCNT/TiO_2 epoxy (High magnification of mirror zone), (c1) MWCNT/APTES epoxy, and (c2) MWCNT/APTES epoxy (High magnification of mirror zone).

3.4. Dynamic Mechanical Properties of Neat Epoxy and Its Nanocomposites

The effect of dispersion and loading of different types MWCNTs in epoxy for Storage modulus (an indicator for elastic properties) has been shown in **Figure 7**. The figure shows that the storage modulus is strongly influenced by the dispersion and type of MWCNTs. The storage modulus of MWCNT/TiO_2 epoxy nanocomposite increases with 1.5 wt.% loading of MWCNT/TiO_2 at below the glass transition temperature (Tg). The reinforcement of MWCNT/TiO_2 leads to 19% enhancement in storage modulus respectively at temperature 35˚C (**Table 1**) in comparison with neat epoxy. This improvement in storage modulus can be attributed due to cluster free nano level homogeneous dispersion of MWCNT/TiO_2 in entire epoxy matrix (**Figure 7**), which makes available more sites for interaction between MWCNT/TiO_2 and epoxy matrix. It is also an indicator of improvement in stiffness of MWCNT/TiO_2 epoxy nanocomposite in the range of glassy regions. The uniform distribution of MWCNT/TiO_2 in three-dimension epoxy network

may diminish the mobility of epoxy chain network and strongly affect the elastic response below glass transition temperature. But with same loading of MWCNT/APTES, the storage modulus comparatively not so much improved due to incapability of MWCNT/APTES de-agglomeration (Figure 7). As a result, movement of epoxy chain increase, that resulted in reduction of storage modulus. As temperature rises from glass transition region to rubbery region, the storage modulus slightly decreases and then suddenly declined. As the temperature reaches above 110˚C, the storage modulus is not significantly effect by loading of any types of MWCNTs (Figure 7). In this region the reinforcement of MWCNTs have not enough influence for performance of nanocomposites [39] [40]. This may arise due to relatively higher movement of epoxy chain in rubbery region.

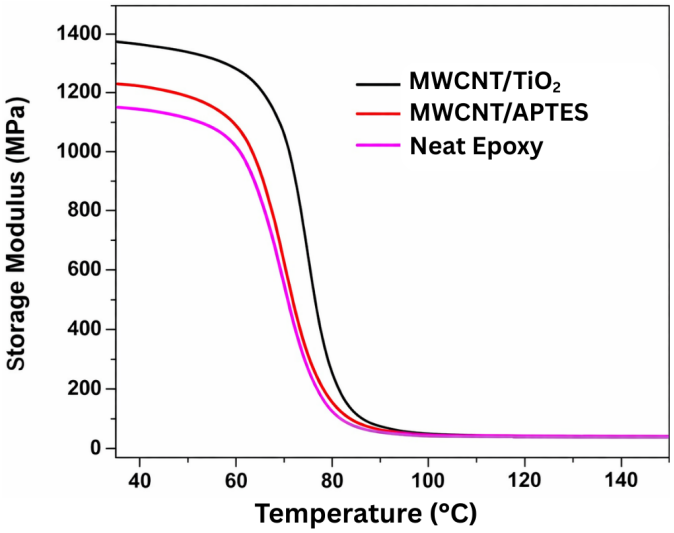

Figure 7. Storage modulus of neat epoxy, MWCNT/APTES epoxynanocomposite and MWCNT/TiO_2 epoxynanocomposite (1.5 wt.%).

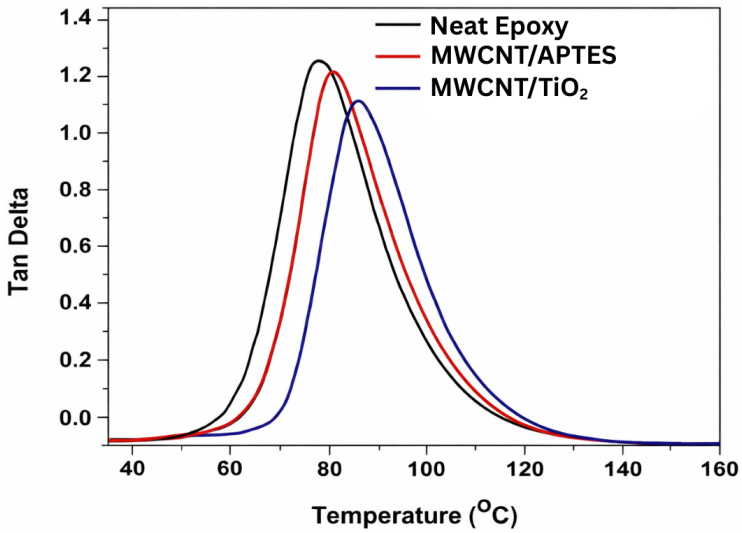

Figure 8. Tan δ vs. temperature of neat epoxy, MWCNT/APTES epoxynanocomposite and MWCNT/TiO_2 epoxynanocomposite (1.5 wt.%).

The ratio of loss modulus to storage modulus is defined as loss factor or tan δ, which indicate the damping behavior of nanocomposite. The temperature corresponding to peak of tan δ curve was treated as glass transition temperature (T_g) of nanocomposite. The effect of the addition of different types of MWCNTs on glass transition temperature of epoxy nanocomposite materials has been shown in Figure 8 and in Table 1. Enhancement in T_g is most prominent for the MWCNT/TiO_2 epoxy where T_g become 84˚C in comparison of neat epoxy with T_g 75˚C (Table 1) The superior dispersion of MWCNT/TiO_2 in entire epoxy creates hindered relaxation mobility in epoxy segments at interface region and resulting in rise of T_g. However, in the case of MWCNT/APTES there in no significant change in glass transition temperature that indicates lower crosslinking density and higher chain mobility. Further, Figure 8 shows a gradual decrease in tan δ peak height with the addition of MWCNTs. This indicates the raise in stiffness of epoxy due to good interfacial interaction between well-dispersed MWCNTs and epoxy matrix. The reduction in tan δ peak height is most prominent for the MWCNT/TiO_2 epoxy nanocomposite.

4. Conclusion

The decoration of MWCNT by TiO_2 nanoparticles significantly improves the dispersion of MWCNTs and assists in generation of homogeneous distribution of MWCNTs in the epoxy matrix. FESEM image showed that TiO_2 nanoparticles were uniformly distributed in epoxy. However, there is a little effect of 1.5 wt.% of TiO_2 on mechanical properties of epoxy. MWCNT/TiO_2 hybrid-epoxy nanocomposite exhibits superior mechanical and anti-corrosion performance. This improvement in performance originates from the synergistic effect of MWCNTs and TiO_2 nanoparticles.

Conflicts of Interest

The authors declare no conflicts of interest regarding the publication of this paper.

References

[1] Xie, S., Li, W., Pan, Z., Chang, B. and Sun, L. (2000) Mechanical and Physical Properties on Carbon Nanotube. *Journal of Physics and Chemistry of Solids*, **61**, 1153-1158. https://doi.org/10.1016/s0022-3697(99)00376-5

[2] Wei, B.Q., Vajtai, R. and Ajayan, P.M. (2001) Reliability and Current Carrying Capacity of Carbon Nanotubes. *Applied Physics Letters*, **79**, 1172-1174. https://doi.org/10.1063/1.1396632

[3] Wong, E.W., Sheehan, P.E. and Lieber, C.M. (1997) Nanobeam Mechanics: Elasticity, Strength, and Toughness of Nanorods and Nanotubes. *Science*, **277**, 1971-1975. https://doi.org/10.1126/science.277.5334.1971

[4] Thostenson, E., Li, C. and Chou, T. (2005) Nanocomposites in Context. *Composites Science and Technology*, **65**, 491-516. https://doi.org/10.1016/j.compscitech.2004.11.003

[5] Iijima, S. (1991) Helical Microtubules of Graphitic Carbon. *Nature*, **354**, 56-58.

https://doi.org/10.1038/354056a0

[6] Baughman, R.H., Zakhidov, A.A. and de Heer, W.A. (2002) Carbon Nanotubes—The Route toward Applications. *Science*, **297**, 787-792. https://doi.org/10.1126/science.1060928

[7] Tang, Z.K., Zhang, L., Wang, N., Zhang, X.X., Wen, G.H., Li, G.D., *et al.* (2001) Superconductivity in 4 Angstrom Single-Walled Carbon Nanotubes. *Science*, **292**, 2462-2465. https://doi.org/10.1126/science.1060470

[8] Thostenson, E.T., Ren, Z. and Chou, T. (2001) Advances in the Science and Technology of Carbon Nanotubes and Their Composites: A Review. *Composites Science and Technology*, **61**, 1899-1912. https://doi.org/10.1016/s0266-3538(01)00094-x

[9] Curtin, W.A. and Sheldon, B.W. (2004) CNT-Reinforced Ceramics and Metals. *Materials Today*, **7**, 44-49. https://doi.org/10.1016/s1369-7021(04)00508-5

[10] Mutiso, R.M. and Winey, K.I. (2015) Electrical Properties of Polymer Nanocomposites Containing Rod-Like Nanofillers. *Progress in Polymer Science*, **40**, 63-84. https://doi.org/10.1016/j.progpolymsci.2014.06.002

[11] Bauhofer, W. and Kovacs, J.Z. (2009) A Review and Analysis of Electrical Percolation in Carbon Nanotube Polymer Composites. *Composites Science and Technology*, **69**, 1486-1498. https://doi.org/10.1016/j.compscitech.2008.06.018

[12] Maktedar, S.S., Malik, P., Avashthi, G. and Singh, M. (2017) Dispersion Enhancing Effect of Sonochemically Functionalized Graphene Oxide for Catalysing Antioxidant Efficacy of Curcumin. *Ultrasonics Sonochemistry*, **39**, 208-217. https://doi.org/10.1016/j.ultsonch.2017.04.006

[13] Maktedar, S.S., Avashthi, G. and Singh, M. (2017) Ultrasound Assisted Simultaneous Reduction and Direct Functionalization of Graphene Oxide with Thermal and Cytotoxicity Profile. *Ultrasonics Sonochemistry*, **34**, 856-864. https://doi.org/10.1016/j.ultsonch.2016.07.016

[14] Maktedar, S.S., Mehetre, S.S., Avashthi, G. and Singh, M. (2017) In Situ Sonochemical Reduction and Direct Functionalization of Graphene Oxide: A Robust Approach with Thermal and Biomedical Applications. *Ultrasonics Sonochemistry*, **34**, 67-77. https://doi.org/10.1016/j.ultsonch.2016.05.015

[15] Maktedar, S.S., Avashthi, G. and Singh, M. (2016) Understanding the Significance of O-Doped Graphene Towards Biomedical Applications. *RSC Advances*, **6**, 114264-114275. https://doi.org/10.1039/c6ra23416j

[16] Mehetre, S.S., Maktedar, S.S. and Singh, M. (2016) Understanding the Mechanism of Surface Modification through Enhanced Thermal and Electrochemical Stabilities of N-Doped Graphene Oxide. *Applied Surface Science*, **366**, 514-522. https://doi.org/10.1016/j.apsusc.2016.01.108

[17] Spitalsky, Z., Tasis, D., Papagelis, K. and Galiotis, C. (2010) Carbon Nanotube-Polymer Composites: Chemistry, Processing, Mechanical and Electrical Properties. *Progress in Polymer Science*, **35**, 357-401. https://doi.org/10.1016/j.progpolymsci.2009.09.003

[18] Fiedler, B., Gojny, F.H., Wichmann, M.H.G., Nolte, M.C.M. and Schulte, K. (2006) Fundamental Aspects of Nano-Reinforced Composites. *Composites Science and Technology*, **66**, 3115-3125. https://doi.org/10.1016/j.compscitech.2005.01.014

[19] Park, S. and Ruoff, R.S. (2009) Chemical Methods for the Production of Graphenes. *Nature Nanotechnology*, **4**, 217-224. https://doi.org/10.1038/nnano.2009.58

[20] Peigney, A., Laurent, C., Flahaut, E., Bacsa, R.R. and Rousset, A. (2001) Specific Surface Area of Carbon Nanotubes and Bundles of Carbon Nanotubes. *Carbon*, **39**, 507-

514. https://doi.org/10.1016/s0008-6223(00)00155-x

[21] Tasis, D., Tagmatarchis, N., Bianco, A. and Prato, M. (2006) Chemistry of Carbon Nanotubes. *Chemical Reviews*, **106**, 1105-1136. https://doi.org/10.1021/cr050569o

[22] Jiménez-Suárez, A., Campo, M., Gaztelumendi, I., Markaide, N., Sánchez, M. and Ureña, A. (2013) The Influence of Mechanical Dispersion of MWCNT in Epoxy Matrix by Calendering Method: Batch Method versus Time Controlled. *Composites Part B*: *Engineering*, **48**, 88-94. https://doi.org/10.1016/j.compositesb.2012.12.011

[23] Pegel, S., Pötschke, P., Petzold, G., Alig, I., Dudkin, S.M. and Lellinger, D. (2008) Dispersion, Agglomeration, and Network Formation of Multiwalled Carbon Nanotubes in Polycarbonate Melts. *Polymer*, **49**, 974-984. https://doi.org/10.1016/j.polymer.2007.12.024

[24] Lachman, N. and Daniel Wagner, H. (2010) Correlation between Interfacial Molecular Structure and Mechanics in CNT/Epoxy Nano-Composites. *Composites Part A*: *Applied Science and Manufacturing*, **41**, 1093-1098. https://doi.org/10.1016/j.compositesa.2009.08.023

[25] Thostenson, E.T. and Chou, T. (2002) Aligned Multi-Walled Carbon Nanotube-Reinforced Composites: Processing and Mechanical Characterization. *Journal of Physics D*: *Applied Physics*, **35**, L77-L80. https://doi.org/10.1088/0022-3727/35/16/103

[26] Guadagno, L., Naddeo, C., Vittoria, V., Sorrentino, A., Vertuccio, L., Raimondo, M., *et al.* (2010) Cure Behavior and Physical Properties of Epoxy Resin—Filled with Multiwalled Carbon Nanotubes. *Journal of Nanoscience and Nanotechnology*, **10**, 2686-2693. https://doi.org/10.1166/jnn.2010.1417

[27] Schulz, S.C., Faiella, G., Buschhorn, S.T., Prado, L.A.S.A., Giordano, M., Schulte, K., *et al.* (2011) Combined Electrical and Rheological Properties of Shear Induced Multiwall Carbon Nanotube Agglomerates in Epoxy Suspensions. *European Polymer Journal*, **47**, 2069-2077. https://doi.org/10.1016/j.eurpolymj.2011.07.022

[28] Grunlan, J.C., Mehrabi, A.R., Bannon, M.V. and Bahr, J.L. (2004) Water-Based Single-Walled-Nanotube-Filled Polymer Composite with an Exceptionally Low Percolation Threshold. *Advanced Materials*, **16**, 150-153. https://doi.org/10.1002/adma.200305409

[29] Zhu, J., Kim, J., Peng, H., Margrave, J.L., Khabashesku, V.N. and Barrera, E.V. (2003) Improving the Dispersion and Integration of Single-Walled Carbon Nanotubes in Epoxy Composites through Functionalization. *Nano Letters*, **3**, 1107-1113. https://doi.org/10.1021/nl0342489

[30] Zhang, Z.Q., Liu, B., Chen, Y.L., Jiang, H., Hwang, K.C. and Huang, Y. (2008) Mechanical Properties of Functionalized Carbon Nanotubes. *Nanotechnology*, **19**, Article ID: 395702. https://doi.org/10.1088/0957-4484/19/39/395702

[31] Liao, Y., Marietta-Tondin, O., Liang, Z., Zhang, C. and Wang, B. (2004) Investigation of the Dispersion Process of SWNTs/SC-15 Epoxy Resin Nanocomposites. *Materials Science and Engineering*: *A*, **385**, 175-181. https://doi.org/10.1016/j.msea.2004.06.031

[32] Kumar, A., Ghosh, P.K., Yadav, K.L. and Kumar, K. (2017) Thermo-Mechanical and Anti-Corrosive Properties of MWCNT/Epoxy Nanocomposite Fabricated by Innovative Dispersion Technique. *Composites Part B*: *Engineering*, **113**, 291-299. https://doi.org/10.1016/j.compositesb.2017.01.046

[33] Muthoosamy, K. and Manickam, S. (2017) State of the Art and Recent Advances in the Ultrasound-Assisted Synthesis, Exfoliation and Functionalization of Graphene Derivatives. *Ultrasonics Sonochemistry*, **39**, 478-493.

https://doi.org/10.1016/j.ultsonch.2017.05.019

[34] Shukla, V., Raval, B. and Singh, M. (2017) Impact of Newly Synthesized Water Soluble Photoluminescent ZNs-L-Cysteine: Core-Shell Nanoparticles in Defining the *In-Situ* Opto-Electronic Orbital Model. *Advanced Materials Letters*, **8**, 156-162. https://doi.org/10.5185/amlett.2017.7078

[35] Mallakpour, S., Abdolmaleki, A. and Azimi, F. (2017) Ultrasonic-assisted Biosurface Modification of Multi-Walled Carbon Nanotubes with Thiamine and Its Influence on the Properties of PVC/TM-MWCNTs Nanocomposite Films. *Ultrasonics Sonochemistry*, **39**, 589-596. https://doi.org/10.1016/j.ultsonch.2017.05.028

[36] Mallakpour, S. and khodadadzadeh, L. (2018) Ultrasonic-Assisted Fabrication of Starch/MWCNT-Glucose Nanocomposites for Drug Delivery. *Ultrasonics Sonochemistry*, **40**, 402-409. https://doi.org/10.1016/j.ultsonch.2017.07.033

[37] Mallakpour, S. and Rashidimoghadam, S. (2018) Application of Ultrasonic Irradiation as a Benign Method for Production of Glycerol Plasticized-Starch/Ascorbic Acid Functionalized MWCNTs Nanocomposites: Investigation of Methylene Blue Adsorption and Electrical Properties. *Ultrasonics Sonochemistry*, **40**, 419-432. https://doi.org/10.1016/j.ultsonch.2017.07.032

[38] Azami, M., Haghighi, M. and Allahyari, S. (2018) Sono-Precipitation of Ag_2CrO_4-C Composite Enhanced by Carbon-Based Materials (AC, GO, CNT and C_3N_4) and Its Activity in Photocatalytic Degradation of Acid Orange 7 in Water. *Ultrasonics Sonochemistry*, **40**, 505-516. https://doi.org/10.1016/j.ultsonch.2017.07.043

[39] Ghosh, P.K., Patel, A. and Kumar, K. (2016) Adhesive Joining of Copper Using Nano-Filler Composite Adhesive. *Polymer*, **87**, 159-169. https://doi.org/10.1016/j.polymer.2016.02.006

[40] Jeon, H., Park, J. and Shon, M. (2013) Corrosion Protection by Epoxy Coating Containing Multi-Walled Carbon Nanotubes. *Journal of Industrial and Engineering Chemistry*, **19**, 849-853. https://doi.org/10.1016/j.jiec.2012.10.030